[10] D. Zanotto, G. Rosati, and S. K. Agrawal, "Modeling and control of a 3-DOF pendulum-like manipulator," in *Proc. IEEE Int. Conf. Robot. Autom.*, Shanghai, China, May 9–13, 2011, pp. 3964–3969.
[11] N. Zoso and C. Gosselin, "Point-to-point motion planning of a parallel 3-DOF underactuated cable-suspended robot," in *Proc. IEEE Int. Conf. Robot. Autom.*, St. Paul, MN, USA, May 14–18, 2012, pp. 2325–2330.
[12] G. Barrette and C. Gosselin, "Determination of the dynamic workspace of cable-driven planar parallel mechanisms," *ASME J. Mech. Design*, vol. 127, no. 2, pp. 242–248, 2005.
[13] C. Gosselin, P. Ren, and S. Foucault, "Dynamic trajectory planning of a two-DOF cable-suspended parallel robot," in *Proc. IEEE Int. Conf. Robot. Autom.*, St. Paul, MN, USA, pp. 1476–1481, May 14–18, 2012.
[14] C. Gosselin, "Global planning of dynamically feasible trajectories for three-dof spatial cable-suspended parallel robots," in *Proc. 1st Int. Conf. Cable-Driven Parallel Robots*, Stuttgart, Germany, Sep. 2–4, 2012, pp. 3–22.
[15] C. Gosselin and A. Hadj-Messaoud, "Automatic planning of smooth trajectories for pick-and-place operations," *ASME J. Mech. Design*, vol. 115, no. 3, pp. 450–456, 1993.

A New Nonlinear Model of Contact Normal Force

Morteza Azad and Roy Featherstone

***Abstract*—This paper presents a new nonlinear model of the normal force that arises during compliant contact between two spheres, or between a sphere and a flat plate. It differs from a well-known existing model by only a single term. The advantage of the new model is that it accurately predicts the measured values of the coefficient of restitution between spheres and plates of various materials, whereas other models do not.**

***Index Terms*—Animation and simulation, compliant contact model, nonlinear damping, normal force.**

I. Introduction

Since robots usually make contact with their environment during the execution of their tasks (e.g., grasping, walking, rolling, etc.), modeling the contact is an unavoidable part of most studies in this field. Two major forces appear during contact: the normal force and the friction force. In this paper, we focus on the normal force and introduce a new model for calculating it. This new model agrees well with existing measurements of the coefficient of restitution between spheres and plates of various materials.

Contact models can be classified into two types: rigid and compliant [3]. The model presented in this paper is compliant. The key difference is that compliant models assume a small amount of local deformation at the contact, which allows the contact forces to be expressed as functions of local position and velocity variables. This feature makes it relatively easy to incorporate a compliant contact model into a dynamics simulator.

Most previous studies of compliant contact models have considered the contact between two spheres, or between a sphere and a flat plate [2], [5], [8], [10]. For example, Hunt and Crossley [5] modeled the ground as a nonlinear spring–damper pair at the contact point with the sphere,

Manuscript received August 1, 2013; accepted November 21, 2013. Date of publication December 19, 2013; date of current version June 3, 2014. This paper was recommended for publication by Associate Editor J. Dai and Editor B. J. Nelson upon evaluation of the reviewers' comments.

M. Azad is with the School of Engineering, The Australian National University, Canberra, Acton, A.C.T. 0200, Australia (e-mail: morteza.azad@anu.edu.au).

R. Featherstone is a Visiting Professor with the Department Advanced Robotics, Istituto Italiano di Tecnologia, Genova 16163, Italy (e-mail: roy.featherstone@ieee.org).

Digital Object Identifier 10.1109/TRO.2013.2293833

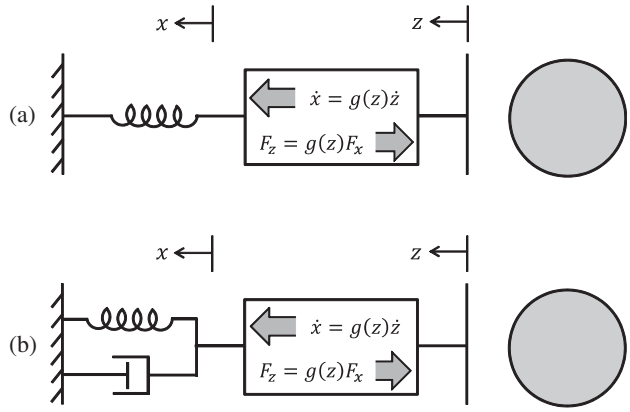

Fig. 1. Nonlinear (a) elastic and (b) viscoelastic models of contact in which the nonlinearity is encapsulated in a gearbox with a position-dependent gear ratio of $g(z)$.

and introduced a nonlinear equation for the normal force between a sphere and the ground as

$$F = kz^n + \lambda z^p \dot{z}^q \tag{1}$$

where z is the deformation variable, which is defined as the penetration distance of the undeformed sphere into the undeformed ground, $\dot{z}$ is the rate of deformation, k and λ are the coefficients of the spring and damper, respectively, and n, p, and q are constant parameters. They chose the values of these parameters as $n = \frac{3}{2}$ (to get similar results to Hertz's theory [6]), $p = \frac{3}{2}$, and $q = 1$ (to be able to determine the value of λ with respect to k conveniently), resulting in the equation

$$F = kz^{\frac{3}{2}} + \lambda z^{\frac{3}{2}} \dot{z}. \tag{2}$$

This model has since appeared in [8] and [10], and has become well known in the robotics community. We shall refer to it as the Hunt/Crossley model. Following a different line of reasoning, Lee and Wang [9] obtained a model identical to (2), but with $p = 1$ instead of $\frac{3}{2}$. Our new model also differs from (2) only in the value of p, which we show has to be $p = \frac{1}{2}$.

In the remainder of this paper, we first derive the new model and then test it against experimentally measured values of the coefficient of restitution between spheres and plates of various materials. It is shown that the new model accurately fits the experimental data, whereas the Hunt/Crossley model does not. The new model is based on an idea that appeared originally in [1], which studied the contact between a rigid sphere and a compliant plate.

II. Contact Force Model

The contact force in (1) is the sum of an elastic component and a dissipative component. The expression $kz^{\frac{3}{2}}$ in (2) is the elastic force predicted by Hertz's theory for contact between a sphere and a plate, and is known to be correct. As Hertz's theory is based on an assumption of linear elasticity in the contacting solids, it follows that the nonlinearity in the elastic force expression is due to the nonlinear geometry at the contact (i.e., the curved surface of the sphere).

We can model the elastic contact force with a linear spring and a nonlinear gearbox, as shown in Fig. 1(a). The spring represents the lumped elasticity of the contacting bodies, and its stiffness K depends on the material properties of the contacting bodies. The gearbox has a deformation-dependent gear ratio of $g(z)$ and represents the nonlinear variation of contact area and strain distribution with z.

This model works as follows. A displacement z at the contact causes a displacement x of the spring, which in turn causes a spring force of $F_x = Kx$. This force is transmitted back through the gearbox, resulting in a force of $F_z = g(z)F_x$ at the contact. The relationship between z and x is obtained via the velocity equation $\dot{x} = g(z)\dot{z}$, which implies that $x = \int_0^z g(z)dz$. Thus, the elastic force that is produced by this model is

$$F_z = g(z)K\int_0^z g(z)\,dz. \tag{3}$$

On comparing this with the desired value $F_z = kz^{\frac{3}{2}}$, it can be seen that

$$g(z) = Cz^{\frac{1}{4}} \tag{4}$$

where C is a constant that depends on the radius of the sphere. This value for $g(z)$ implies $k = 4C^2K/5$. However, instead of using K and C, it is better to obtain k directly from Hertz's theory, which gives

$$k = \frac{4}{3}E^*\sqrt{R} \tag{5}$$

where

$$\frac{1}{E^*} = \frac{1-\nu_1^2}{E_1} + \frac{1-\nu_2^2}{E_2}. \tag{6}$$

E_1 and E_2 are the moduli of elasticity of the contacting bodies, and ν_1 and ν_2 are their Poisson ratios [6].

To obtain the new model, we simply replace the linear spring in Fig. 1(a) with a spring–damper pair, as shown in Fig. 1(b). In physical terms, this amounts to replacing the assumption of linear elasticity in the contacting bodies with an assumption of linear viscoelasticity, while keeping the contact geometry the same. The contact normal force that is generated by this model is

$$F_z = g(z)\Big(K\int_0^z g(z)\,dz + Dg(z)\dot{z}\Big) \tag{7}$$

where D is the damper coefficient, which depends on the material properties of the contacting bodies. Substituting (4) into this equation gives

$$F_z = kz^{\frac{3}{2}} + \lambda z^{\frac{1}{2}}\dot{z} \tag{8}$$

where $\lambda = C^2D$. This is the equation for the new model. Observe that it differs by only a single exponent from (2). We do not have a formula for λ equivalent to the formula for k in (5), but it is clear that λ and k must have the same dependence on R; therefore, we can at least say that

$$\lambda = \lambda^*\sqrt{R} \tag{9}$$

where λ^* is independent of R.

The progression from a lumped-elastic model, as in Fig. 1(a), to a lumped-viscoelastic model, as in Fig. 1(b), requires one extra assumption: either the two materials have the same recovery time constant (the ratio D/K locally in each material), or else one material is much harder than the other so that substantially all of the compression takes place in the softer body. Although this assumption is theoretically necessary for (8) to be physically valid, we have found that in practice (8) still gives good results even when this assumption does not hold, although the results are less accurate than when the assumption does hold.

A. Equivalent Radius

We now consider a compliant contact between two spheres having radii R_1 and R_2. If z is small compared with the radii, then the local deformation in the contact zone is the same as the local deformation in a compliant contact between a sphere of radius R and a flat plate, where

$$\frac{1}{R} = \frac{1}{R_1} + \frac{1}{R_2}. \tag{10}$$

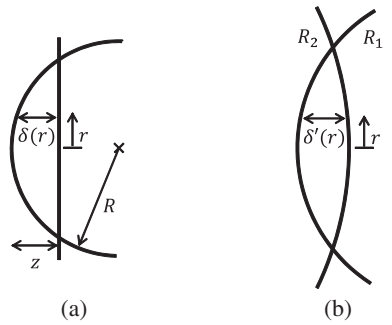

Fig. 2. Local deformation in a contact (a) between a sphere and a flat plate and (b) between two spheres.

We, therefore, call R the equivalent radius of the contact.

Fig. 2 illustrates this result. Let $\delta(r)$ denote the local deformation in the sphere–plate contact at a distance of r from the center of the contact zone [so $\delta(0) = z$], and let $\delta'(r)$ be the same function for the sphere–sphere contact. If the three radii satisfy (10), then $\delta(r) - \delta'(r)$ is $o(z^2)$, meaning that the difference between $\delta(r)$ and $\delta'(r)$ converges to zero in proportion to z^2 as z goes to zero.

Thus, the contact model in (8) applies equally to a sphere–plate contact and to a sphere–sphere contact. In the latter case, one uses the equivalent radius in (5) and (9).

B. Practical Implementation

If a dynamics simulator is to implement a compliant contact model both efficiently and accurately, then it needs the following features: 1) the ability to determine accurately the moment when a contact is made or broken, and ensure that the current integration step ends precisely at that moment, and 2) the ability to vary the integration step size so that tiny steps can be taken during the few milliseconds when the accelerations are very large, and bigger steps at other times. Simulink has these features, but many other simulators do not. A simulator lacking these features can still do the job, but it will be suboptimal.

The simplest practical implementation of (8) is

$$F_z = \begin{cases} 0, & \text{if } z \le 0 \\ \max(0, \sqrt{z}\,(kz + \lambda\dot{z})), & \text{if } z > 0 \end{cases} \tag{11}$$

where z and $\dot{z}$ are inputs and F_z is the output. The simulator should interpret $F_z > 0$ as contact, and $F_z = 0$ as no contact. The values of z and $\dot{z}$ are computed from the position and velocity variables of a particular pair of bodies that may make and/or lose contact during the course of the simulation. z will be negative whenever the undeformed shapes of these two bodies do not touch.

Observe that (11) does not use a state variable. Statelessness is regarded as a desirable attribute in a contact model, but there is a small price to pay. In the moments immediately following a loss of contact, the recovery to zero of the spring and damper ought to be modeled using the equation $Kx + D\dot{x} = 0$ with the initial condition $x(t_c) = x_c$, where t_c is the moment of contact loss and x_c is the value of x (computed from z) at that moment. However, to do this would mean treating x as a state variable. Instead, the model in (11) implicitly defines x as $x = \int_0^{\max(z,0)} g(z)\,dz$. The error involved in this approximation is practically zero under all circumstances except when a new contact begins almost immediately after the preceding contact loss. Physically, this could happen on the last bounce before the two bodies settle into continuous contact.

C. Integration Step Size

A common objection to compliant contact models is that they are inefficient because the high stiffness of the contact makes the integration step size too small. To investigate this issue, we performed the following experiment in Simulink: a sphere of mass 66 g is dropped onto a horizontal plate from a height of 1 m, with gravity set at 10 m/s^2 and the contact modeled by (11) with $k = 10^{10}$ and $\lambda = 10^5$. These values are close to the parameters for case B in Fig. 5, which involves a steel sphere striking a cast iron plate—a much stiffer contact than a roboticist would normally want to model. We used Simulink's ode23t (trapezoidal rule) with a relative tolerance of 10^{-5} and a maximum step size of 0.01 s, and ran the simulation for 5 s.

The results are as follows. It takes 2.4 s for the bounce heights to decay to 1 mm, during which time the integrator takes 958 steps implying an average step size of 2.5 ms. During this period, the integrator takes large steps, while the sphere is in flight, and much smaller ones while it is bouncing. It then takes a further 0.2 s for the sphere to settle, during which time the integrator takes another 887 steps implying an average step size of 0.23 ms. Twenty-six microscopic bounces take place during this period (which is physically realistic) and the resonant frequency in the limit is 1.4 kHz. These are both consequences of the contact being extremely stiff. Finally, the integrator takes a further 255 steps during the remaining 2.4 s, implying an average step size of 9.4 ms.

These figures show that, even for an extremely stiff contact, the integrator needs to take small steps only for very brief periods, such as during individual bounces or during the transition from bouncing to the steady contact. With softer materials, such as aluminum or plastic, the contact would be less stiff and the integrator would of course take bigger steps.

To put these figures into context, in a typical robot dynamics simulator, the control system is modeled as a program that repeatedly samples its inputs, performs a calculation, and modifies its outputs. The rate at which the control system does this determines the maximum integration step size. For example, if the control system runs at a rate of 1 kHz, which is not unusual, then the maximum integration step size will be 1 ms. In this context, it can be seen that the use of a compliant contact model is unlikely to cause a significant reduction in the overall computational efficiency.

III. Coefficient of Restitution

In this section, we compare the new model's predictions of the coefficient of restitution with those of other models, and with published experimental results. For each model, the predicted coefficients of restitution are obtained via accurate dynamics simulations implemented in Simulink and, therefore, reflect each model's behavior in a simulation context.

According to experiments reported by Goldsmith [4] on measuring the coefficient of restitution for impacts between spheres and thick plates, the value should decrease as the impact velocity increases. Fig. 3 shows the values of the coefficient of restitution at different impact velocities, as calculated by the new model in (8), the Hunt/Crossley model in (2), and a linear spring–damper model [(1) with $n = q = 1$ and $p = 0$]. In every case, gravity is set to zero. (With nonzero gravity, impacts below a threshold velocity do not result in a bounce, implying a coefficient of restitution equal to zero.) As can be seen, the linear model predicts a constant coefficient of restitution, which is not physically realistic. The two nonlinear models correctly predict a decrease in the coefficient of restitution with the increasing impact velocity, and they predict curves with different shapes. The difference between these curves can be observed more clearly by changing the scale of the horizontal axis to a logarithmic scale, as shown in Fig. 4. It can now be seen that the new model predicts an almost linear relationship between the coefficient of restitution and the logarithm of the impact velocity, whereas the Hunt/Crossley model does not.

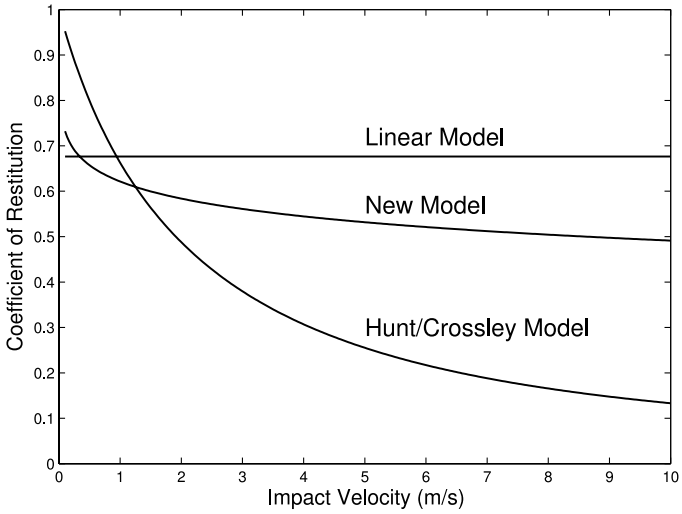

Fig. 3. Examples of coefficient of restitution versus impact velocity calculated by three different models.

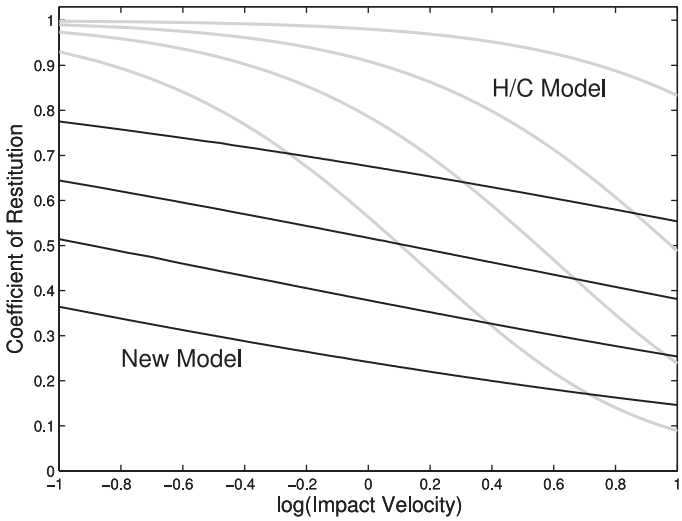

Fig. 4. Coefficient of restitution versus logarithm of impact velocity calculated by the Hunt/Crossley model and the new model for a fixed value of k and different values of λ.

Despite having two independent parameters, each model gives rise to only a one-parameter family of curves of coefficient of restitution versus impact velocity. This is because the two parameters together define two independent properties of the model: the coefficient of restitution and the duration of the contact phase of a bounce. For the new model, it can be shown that, for any $\alpha > 0$, the parameter pair $(\alpha^{-2.5}k, \alpha^{-1.5}\lambda)$ produces the same coefficient of restitution, but α times the duration, as the parameter pair (k, λ). For the Hunt/Crossley model, it is the same except that $\alpha^{-2.5}\lambda$ appears in place of $\alpha^{-1.5}\lambda$. It, therefore, follows that the full variety of possible curves can be obtained by setting k to an arbitrary fixed value and varying λ, which is how we obtained the curves shown in Fig. 4.

Fig. 5 compares the calculated values of the coefficient of restitution according to the new model and the Hunt/Crossley model with empirical results published in [4] and [7], all on a logarithmic scale.

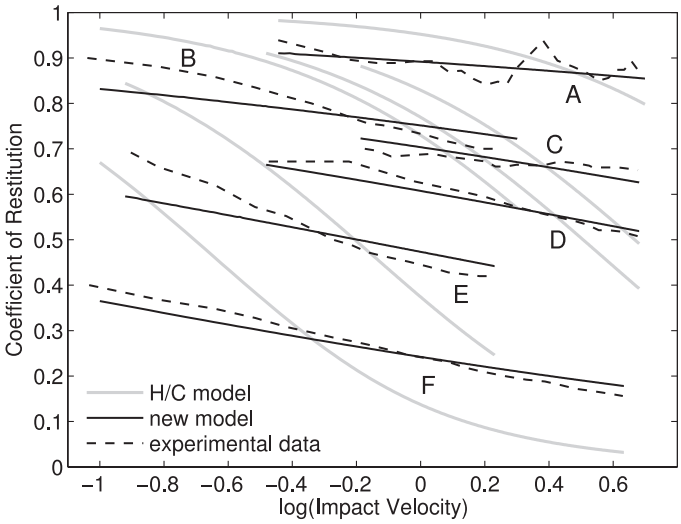

Fig. 5. Coefficient of restitution versus logarithm of impact velocity for the contact between (A) brass spheres ($R_1 = R_2 = 1.5$ cm), (B) a steel sphere ($R = 1.27$ cm) and a cast iron plate, (C) cork spheres ($R_1 = R_2 = 1.66$ cm), (D) a steel sphere ($R = 1.65$ cm) and a cork plate, (E) a steel sphere ($R = 1.27$ cm) and a brass plate, and (F) a steel sphere ($R = 1.27$ cm) and a cold-worked lead plate.

The empirical data were obtained by hand measurements from [4, Fig. 172] and [7, Fig. 3]. The model curves were obtained by calculating k from the appropriate material properties and sphere radius using (5), and tuning λ to obtain a least-squares best fit to the data points. Some of the curves appear to fit the data better at higher velocities than at lower ones, but this is simply a consequence of the distribution of data points along the data curves (more points at the high end because of the logarithmic scale used) and the fact that all data points were weighted equally.

From Fig. 5, we can immediately see that the data follow approximately straight lines, and that the new model fits the data much better than the Hunt/Crossley model. Furthermore, in cases (A), (C), (D), and (F), the model fits the data very well. Although the fit is not so good in cases (B) and (E), it is still better than any fit that can be achieved with either the linear or the Hunt/Crossley model. One possible reason for the less accurate fit in cases (B) and (E) is that these are the two cases in which the sphere and plate are made of different materials having similar stiffnesses; therefore, it is possible that the assumption in Section II does not hold.

It has been frequently assumed in the literature that the coefficient of restitution varies linearly with the impact velocity; for example, in [4], [5], [9], and [10]. However, this is not a good assumption because, as Fig. 5 clearly shows, the coefficient of restitution actually varies linearly with the logarithm of impact velocity.

IV. Conclusion

A new nonlinear model of contact normal force during compliant contact has been presented. It differs by only a single exponent from the well-known model of Hunt and Crossley [5]. However, detailed comparisons between published experimental measurements of the coefficients of restitution between spheres and plates of various materials, and the coefficients of restitution predicted by the new model and the Hunt/Crossley model, show that the new model provides a substantially more accurate fit to the experimental data. It is, therefore, likely to be a better choice when physically accurate simulations are required.

References

[1] M. Azad and R. Featherstone, "Modelling the contact between a rolling sphere and a compliant ground plane," presented at the Australas. Conf. Robot. Autom., Brisbane, Australia, Dec. 1–3, 2010.

[2] E. Falcon, C. Laroche, S. Fauve, and C. Coste, "Behavior of one inelastic ball bouncing repeatedly off the ground," *Eur. Phys. J. B*, vol. 3, pp. 45–57, 1998.

[3] G. Gilardi and I. Sharf, "Literature survey of contact dynamics modelling," *Mech. Mach. Theory*, vol. 37, pp. 1213–1239, 2002.

[4] W. Goldsmith, *Impact: The Theory and Physical Behaviour of Colliding Solids*. London, U.K.: Edward Arnold, 1960.

[5] K. H. Hunt and F. R. E. Crossley, "Coefficient of restitution interpreted as damping in vibroimpact," *J. Appl. Mech.*, vol. 42, no. 2, pp. 440–445, 1975.

[6] K. L. Johnson, *Contact Mechanics*. Cambridge, U.K.: Cambridge Univ. Press, 1977.

[7] G. Kawabara and K. Kono, "Restitution coefficient in a collision between two spheres," *Jpn. J. Appl. Phys.*, vol. 26, no. 8, pp. 1230–1233, 1987.

[8] H. M. Lankarani and P. E. Nikravesh, "A contact force model with hysteresis damping for impact analysis of multi-body systems," *J. Mech. Des.*, vol. 112, no. 3, pp. 369–376, 1990.

[9] T. W. Lee and A. C. Wang, "On the dynamics of intermittent-motion mechanisms—Part 1: Dynamic model and response," *J. Mech., Transmiss. Autom. Des.*, vol. 105, no. 3, pp. 534–540, 1983.

[10] D. W. Marhefka and D. E. Orin, "A compliant contact model with nonlinear damping for simulation of robotic systems," *IEEE Trans. Syst., Man, Cybern. A, Syst., Humans*, vol. 29, no. 6, pp. 566–572, Nov. 1999.

Leader–Follower Coordinated Tracking of Multiple Heterogeneous Lagrange Systems Using Continuous Control

Ziyang Meng, Dimos V. Dimarogonas, and Karl H. Johansson

***Abstract*—In this paper, we study the coordinated tracking problem of multiple heterogeneous Lagrange systems with a dynamic leader. Only nominal parameters of Lagrange dynamics are assumed to be available. Under the local interaction constraints, i.e., the followers only have access to their neighbors' information and the leader being a neighbor of only a subset of the followers, continuous coordinated tracking algorithms with adaptive coupling gains are proposed. Except for the benefit of the chattering-free control achieved, the proposed algorithm also has the attribute that it does not require the neighbors' generalized coordinate derivatives. Global asymptotic coordinated tracking is guaranteed, and the tracking errors between the followers and the leader are shown to converge to zero. Examples are given to validate the effectiveness of the proposed algorithms.**

***Index Terms*—Continuous control algorithms, coordinated tracking, multiple heterogeneous Lagrange systems.**

Manuscript received May 8, 2013; revised September 24, 2013; accepted December 2, 2013. Date of publication December 23, 2013; date of current version June 3, 2014. This paper was recommended for publication by Associate Editor P. R. Giordano and Editor G. Oriolo upon evaluation of the reviewers' comments. This work was supported in part by the Knut and Alice Wallenberg Foundation, the Swedish Research Council. A preliminary version of this work was presented at the 52nd IEEE Conference on Decision and Control, Palazzo dei Congressi, Florence, Italy, [19].

The authors are with ACCESS Linnaeus Centre, School of Electrical Engineering, Royal Institute of Technology, Stockholm 10044, Sweden (e-mail: ziyangm@kth.se; dimos@kth.se; kallej@kth.se).

Color versions of one or more of the figures in this paper are available online at http://ieeexplore.ieee.org.

Digital Object Identifier 10.1109/TRO.2013.2294060